

Fabrication and Characterization of $(1-x)\text{BiFeO}_3\text{-}x\text{BaTiO}_3$ Ceramics Prepared by a Solid State Reaction Method

S. Chandarak^{1*}, M. Unruan², T. Sareein², A. Ngamjarrojana², S. Maensiri³,
P. Laoratanakul⁴, S. Ananta², and R. Yimnirun⁵

¹*School of Ceramic Engineering, Suranaree University of Technology, Nakhon Ratchasima 30000, Thailand*

²*Department of Physics and Materials Science, Faculty of Science, Chiang Mai University, Chiang Mai 50200, Thailand*

³*Department of Physics, Faculty of Science, Khon Kaen University, 40002, Thailand*

⁴*National Metal and Materials Technology Center (MTEC), Pathumthani 12120, Thailand*

⁵*School of Physics, Institute of Science, Suranaree University of Technology, Nakhon Ratchasima 30000, Thailand*

(Received 28 October 2008, Received in final form 9 March 2009, Accepted 11 March 2009)

In this study, $\text{BiFeO}_3\text{-BaTiO}_3$ ceramics have been fabricated by a solid-state reaction method. The effects of BaTiO_3 content in the $(1-x)\text{BiFeO}_3\text{-}x\text{BaTiO}_3$ ($x = 0.1, 0.2, 0.25, 0.3, 0.4, 0.5$) system on crystal structure and magnetic, dielectric, and ferroelectric properties were investigated. Perovskite BiFeO_3 was stabilized through the formation of a solid solution with BaTiO_3 . Rhombohedrally distorted structure $(1-x)\text{BiFeO}_3\text{-}x\text{BaTiO}_3$ ceramics showed strong ferromagnetism at $x = 0.5$. Dielectric and ferroelectric properties of the $\text{BiFeO}_3\text{-BaTiO}_3$ system also changed significantly upon addition of BaTiO_3 . It was found that the maximum dielectric and ferroelectric properties were exhibited in the $(1-x)\text{BiFeO}_3\text{-}x\text{BaTiO}_3$ system at $x = 0.25$. This suggested the morphotropic phase boundary (MPB) with the coexistence of both rhombohedral and cubic phases of the $(1-x)\text{BiFeO}_3\text{-}x\text{BaTiO}_3$ system at $x = 0.25$.

Keywords : BiFeO_3 , BaTiO_3 , ferromagnetism, ferroelectric, dielectric

1. Introduction

Recently, multiferric materials, where both electric and magnetic polarizations coexist, have been extensively studied. This class of materials is considered to offer a large application potential for novel devices by taking advantage of 2 coupled ferric properties based on local off-centered crystal distortion and electron spin [1, 2]. BiFeO_3 is a representative material that shows ferroelectric (T_C : 1103 K) and antiferromagnetic (T_N : 643 K) properties [3-5]. The crystallographic structure of BiFeO_3 is a rhombohedrally distorted perovskite structure [6]. In addition, it is also known to exhibit weak ferromagnetism at room temperature due to a residual moment from a canted spin structure [7, 8]. The spontaneous polarization of BiFeO_3 single crystals has been reported to be $3.5 \mu\text{C}/\text{cm}^2$ along the $\langle 100 \rangle$ direction and $6.1 \mu\text{C}/\text{cm}^2$ along the $\langle 111 \rangle$ direction at 77 K [9]. However, the preparation of pure BiFeO_3 in a bulk form without traces of

impurities has proven a difficult task. Therefore, $\text{BiFeO}_3\text{-ABO}_3$ solid solution systems have attracted great attention as a means to increase structural stability. Furthermore, another serious problem of BiFeO_3 -based ceramics is their low, electrical resistivity, which affects the measurement of ferroelectric (dielectric) properties at ambient temperatures. BaTiO_3 is a prototype ferroelectric material with several excellent ferroelectric properties (T_C : 393 K, P_S : $26 \mu\text{C}/\text{cm}^2$, and $\epsilon_r > 1000$), and is expected that both ferroelectricity and ferromagnetism still coexist in the new compound formed when mixed with BiFeO_3 .

In this work, perovskite $(1-x)\text{BiFeO}_3\text{-}x\text{BaTiO}_3$ ($x = 0, 0.1, 0.2, 0.25, 0.3, 0.4, 0.5$) ceramics were prepared by the solid-state reaction method. Effects of BaTiO_3 content on crystallographic phase, magnetization behavior, and electrical properties of the resultant $(1-x)\text{BiFeO}_3\text{-}x\text{BaTiO}_3$ ceramics were investigated.

2. Experimental Procedure

The $(1-x)\text{BiFeO}_3\text{-}x\text{BaTiO}_3$ ceramics were prepared by a solid-state reaction with conventional milling and firing

*Corresponding author: Tel: +66-44-224472
Fax: +66-53-943445, e-mail: pinky_pure58@hotmail.com

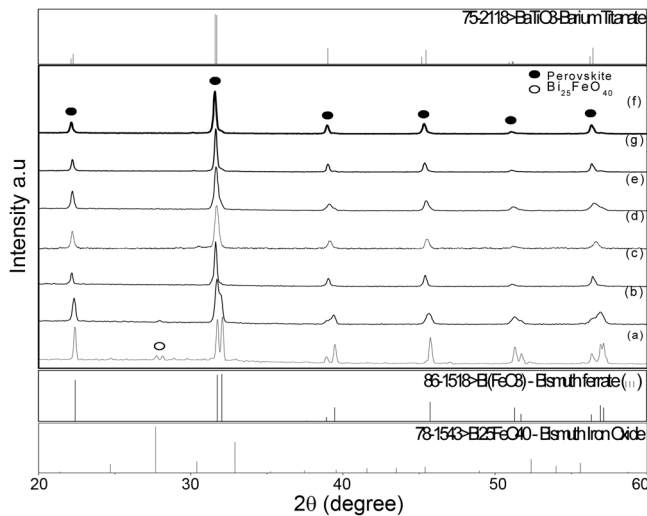


Fig. 1. XRD patterns of $(1-x)\text{BiFeO}_3-x\text{BaTiO}_3$ ceramics: (a) $x = 0$; (b) $x = 0.1$; (c) $x = 0.2$; (d) $x = 0.25$; (e) $x = 0.3$; (f) $x = 0.4$; (g) $x = 0.5$.

techniques. BaCO_3 , TiO_2 , Bi_2O_3 , and Fe_2O_3 powders corresponding to the $(1-x)\text{BiFeO}_3-x\text{BaTiO}_3$ ($x = 0.1, 0.2, 0.25, 0.3, 0.4, 0.5$) were mixed by a conventional ball-milling method for 30 min. The mixtures were dried, pressed, and calcined at 900°C for 5 h at a rate of $5^\circ\text{C}/\text{min}$. The calcined samples were ground and pressed into pellets, with polyvinyl alcohol as the binder. The powder compacts were subsequently sintered at $925\text{--}1050^\circ\text{C}$ for 2 h at heating and cooling rates of $5^\circ\text{C}/\text{min}$.

Crystallographic phase identification of the prepared $(1-x)\text{BiFeO}_3-x\text{BaTiO}_3$ ceramics was performed by X-ray diffraction (XRD) analysis using $\text{CuK}\alpha$ radiation with a monochromator. The magnetization behavior of the $(1-x)\text{BiFeO}_3-x\text{BaTiO}_3$ powder samples was characterized using a vibrating sample magnetometer (VSM). The dielectric properties were evaluated with an impedance gain phase analyzer. The polarization-electric (P-E) hysteresis loop was also measured using the Sawyer-Tower circuit at room temperature.

3. Results and Discussion

3.1. Phase Identification

As shown in Fig. 1, XRD patterns show that $(1-x)\text{BiFeO}_3-x\text{BaTiO}_3$ ($x = 0.1, 0.2, 0.25, 0.3, 0.4, 0.5$) ceramics crystallize in the perovskite single phase, without any second phase like pyrochlore. Conversely, BiFeO_3 ($x = 0$) ceramics crystallized in the perovskite BiFeO_3 with a small amount of $\text{Bi}_{25}\text{FeO}_{40}$ phase, as shown in Fig. 1a. Regarding BiFeO_3 , it has proven a difficult task to prepare a pure compound because of the low structural stability of perovskite BiFeO_3 and its relatively low

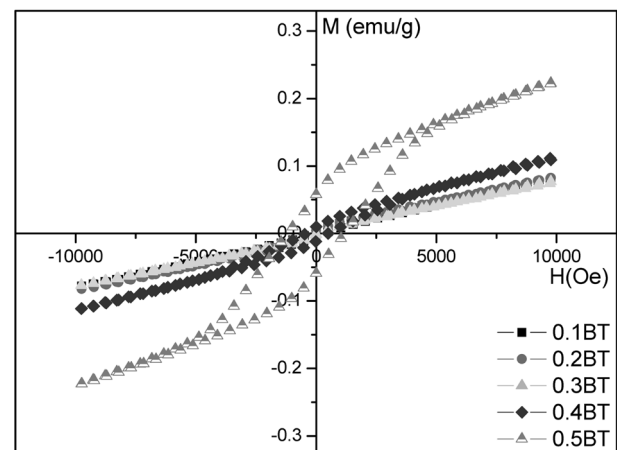


Fig. 2. M-H Hysteresis loops of $(1-x)\text{BiFeO}_3-x\text{BaTiO}_3$ ceramic powders $x = 0.1\text{--}0.5$.

tolerance factor. However, the diffraction lines of the impurity phase disappeared by formation of a solid solution with BaTiO_3 , as shown in Fig. 1(b)–(g). Crystallographic symmetry of $\text{BiFeO}_3\text{--BaTiO}_3$ changed from rhombohedral to cubic near $x = 0.3$. In an earlier report, the crystal structure was rhombohedral between $x = 0$ and 0.33 , cubic between $x = 0.33$ and 0.925 , and tetragonal over $x = 0.925$ [10].

3.2. Magnetic Properties

The magnetization behavior of perovskite $(1-x)\text{BiFeO}_3-x\text{BaTiO}_3$ was evaluated using a VSM. Fig. 2 shows the M-H hysteresis loops of $(1-x)\text{BiFeO}_3-x\text{BaTiO}_3$ ($x = 0.1, 0.2, 0.3, 0.4, 0.5$) crystalline powders measured at room temperature. These powders were prepared by grinding the sintered $(1-x)\text{BiFeO}_3-x\text{BaTiO}_3$ disks. The samples showed typical M-H hysteresis loops of weak ferromagnetism at $x = 0.1, 0.2$, and 0.3 , and stronger ferromagnetism at $x = 0.4$ and 0.5 . The usual polycrystalline BiFeO_3 ceramics showed M-H hysteresis loops without spontaneous magnetization [11]. The onset of ferromagnetism of the BaTiO_3 -rich compositions is thought to depend upon the structural distortion (rhombohedrally distorted crystal structure) [12] and statistical distributions of Fe^{3+} and Ti^{4+} ions in the octahedral sites of $\text{BiFeO}_3\text{--BaTiO}_3$ [13].

3.3. Electrical Properties

The perovskite $(1-x)\text{BiFeO}_3-x\text{BaTiO}_3$ single-phase ceramics were obtained for $x = 0.1, 0.2, 0.25, 0.3, 0.4$, and 0.5 compositions, as described in 3.1. These ceramics also showed high sintered densities near 90% of the theoretical density. Dielectric properties of $(1-x)\text{BiFeO}_3-x\text{BaTiO}_3$ sintered bodies were evaluated at room temperature. However, the insulating resistance of the $x = 0.1, 0.2, 0.25$,

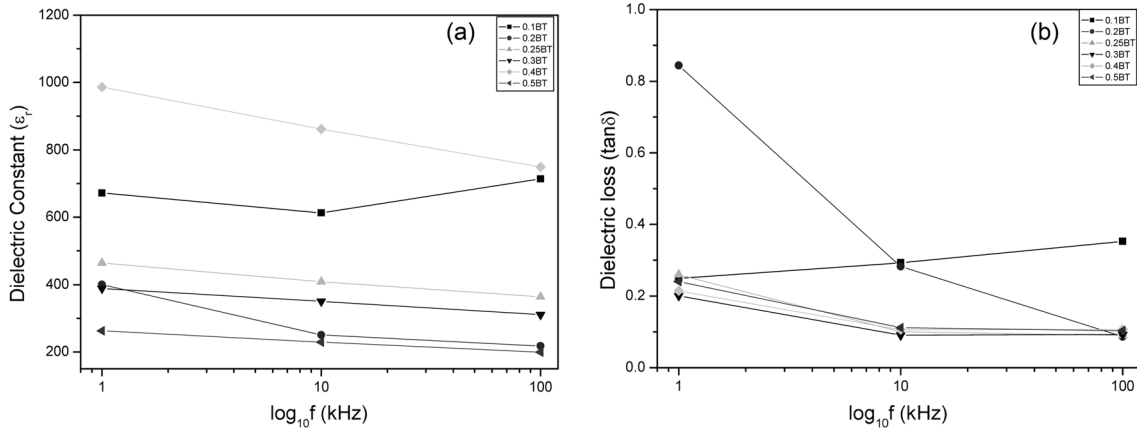


Fig. 3. (a) Dielectric constant and (b) dielectric loss of $(1-x)\text{BiFeO}_3-x\text{BaTiO}_3$ as a function of measuring frequency.

0.3, 0.4, and 0.5 samples was too low to characterize the temperature-dependent dielectric properties, regardless the amount of BaTiO_3 . The values of dielectric loss ($\tan\delta$) of the samples were rather high over a wide frequency range. Among them, the electrical resistivity of the $0.75\text{BiFeO}_3-0.25\text{BaTiO}_3$ sample was $4.7 \times 10^3 \Omega\cdot\text{cm}$.

Fig. 3 shows the frequency dependence of the dielectric constant (ϵ_r) and dielectric loss ($\tan\delta$) for $(1-x)\text{BiFeO}_3-x\text{BaTiO}_3$ ceramics. Higher dielectric constants (ϵ_r) in some composition are possibly due to high dielectric loss ($\tan\delta$). When BaTiO_3 was added, the dielectric constant value increased. However, at $x = 0.5$ composition the dielectric constant decreased because the ceramics were insufficiently sintered (determined from SEM micrographs not shown here and a relatively lower value in density of $< 90\%$ the theoretical density). The insulating resistance of the sample was high at $0.75\text{BiFeO}_3-0.25\text{BaTiO}_3$, suggesting that $0.75\text{BiFeO}_3-0.25\text{BaTiO}_3$ behaves as an acceptor

due to its multivalency and prevents electron hopping ($\text{Fe}^{3+} \rightarrow \text{Fe}^{2+}$) in $(1-x)\text{BiFeO}_3-x\text{BaTiO}_3$. The ϵ_r values of the $\text{BiFeO}_3\text{-BaTiO}_3$ ceramics were approximately 250-650. Higher loss of low frequency 1 kHz may be a result of surface charge conduction that increases the dielectric loss. A decrease of the dielectric properties with increasing frequency is caused by the inability of various polarization contributions to follow the change of the applied electric field, leading to lower dielectric constants and loss at higher frequencies.

Fig. 4 shows the P-E hysteresis loops of $(1-x)\text{BiFeO}_3-x\text{BaTiO}_3$ measured at a frequency of 50 kHz and room temperature. These samples showed typical ferroelectric P-E hysteresis loops at an applied field of 40-50 kV/cm. When BaTiO_3 was added, P-E hysteresis loops of the $(1-x)\text{BiFeO}_3-x\text{BaTiO}_3$ system could be changed. The P-E hysteresis loop at $x = 0.1$ was paraelectric. BaTiO_3 addition helped increase ferroelectric properties. At $x > 0.25$, the hysteresis loops were similar to the BaTiO_3 ceramic, and the remnant polarization decreased, possibly due to samples incompletely sintered (observed from SEM micrographs not shown here and the density of the sinter specimen near $< 90\%$ the theoretical density). The best hysteresis loop was obtained in the $0.75\text{BiFeO}_3-0.25\text{BaTiO}_3$ composition. The remnant polarization (P_r) and coercive field (E_c) (sintered at 925°C) was approximately $12 \mu\text{C}/\text{cm}^2$ and $22 \text{ kV}/\text{cm}$, respectively. However, further improvement of ferroelectric properties is clearly required; therefore, optimization of the $0.75\text{BiFeO}_3-0.25\text{BaTiO}_3$ is currently under investigation.

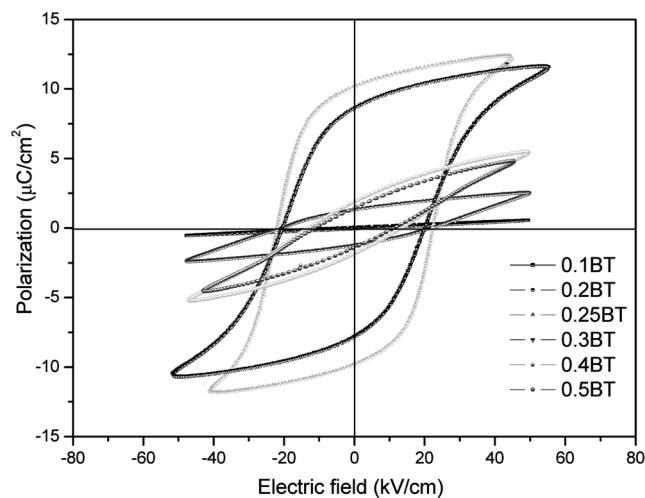


Fig. 4. P-E Hysteresis loops of the $(1-x)\text{BiFeO}_3-x\text{BaTiO}_3$ sample sintered at 925°C .

4. Conclusions

Perovskite $(1-x)\text{BiFeO}_3-x\text{BaTiO}_3$ ceramics were successfully prepared by the solid-state reaction method. In this system, impurity peaks of a second phase disappeared by

formation of a solid solution with BaTiO₃. Perovskite BiFeO₃ was then stabilized through the formation of a solid solution with BaTiO₃. Rhombohedrally distorted structure (1-x)BiFeO₃-xBaTiO₃ ceramics showed strong ferromagnetism at $x = 0.5$. Dielectric and ferroelectric properties of the BiFeO₃-BaTiO₃ system also changed significantly with BaTiO₃ content. It was found that the maximum dielectric and ferroelectric properties were exhibited in the (1-x)BiFeO₃-xBaTiO₃ system at $x = 0.25$, suggesting the morphotropic phase boundary (MPB) (consisting of both rhombohedral and cubic phases) of the (1-x)BiFeO₃-xBaTiO₃ system at $x = 0.25$.

Acknowledgments

This work was financially supported by the Industry/University Cooperative Research Center (I/UCRC) in HDD Component, the Faculty of Engineering, Khon Kaen University and National Electronics and Computer Technology Center, National Science and Technology Development Agency (NSTDA). The author (S.C.) is also thankful to the Synchrotron Light Research Institute (Public Organization) for PhD scholarship.

References

- [1] W. Eerenstein, N. D. Mathur, and J. F. Scott, *Nature* **442**, 759-65 (2006).
- [2] N. G. Kim, Y. S. Koo, and J. H. Jung, *J. Magnetism* **11**, 164 (2006).
- [3] J. Chang, H. M. Jang, and S. K. Kim, *J. Magnetism* **11**, 108 (2006).
- [4] S. V. Kiselev, R. P. Ozarov, and G. S. Zhdanov, *Sov. Phys. Dokl.* **7**, 742 (1962).
- [5] P. Fishetr, M. Polomska, S. Sosnowska, and M. Szymanski, *J. Phys. C* **13**, 1931 (1980).
- [6] F. Kubel and H. Schmid, *Acta Crystallogr., Sect. B* **46**, 698 (1990).
- [7] I. Sosnowska, T. Peterlin-Newmaier, and E. Steichele, *J. Phys. C* **15**, 4835 (1982).
- [8] G. A. Smolenskii and I. Chupis, *Sov. Phys. Usp.* **25**, 475 (1982).
- [9] J. R. Teague, R. Gerson, and W. J. James, *Solid State Commun.* **8**, 1073 (1970).
- [10] I. H. Ismailzade, R. M. Ismailov, A. I. Alekberov, and F. M. Salaev, *Phys. Stat. Sol. (a)* **68**, K81 (1981).
- [11] A. K. Pradhan, K. Zhang, D. Hunter, J. B. Dadson, G. B. Loutts, P. Bhattacharya, R. Katiyar, J. Zhang, D. J. Sellmyer, U. N. Roy, Y. Cui, and A. Burger, *J. Appl. Phys.* **97**, 093903 (2005).
- [12] M. H. Kumar, S. Srinath, G. S. Kumar, and S. V. Suryanarayana, *J. Magn. Mater.* **188**, 203 (1998).
- [13] G. A. Gehring, *Ferroelectrics* **61**, 275 (1994).